

Charge transport and conductance oscillations in gold island films

M. S. Raven

Department of Electrical and Electronic Engineering, University of Nottingham, University Park, Nottingham NG7 2RD, England

(Received 21 October 1983)

Current-voltage measurements including first- and second-derivative measurements have been obtained from gold island films for temperatures between 10 and 300 K. The experimental results and an empirical analysis of the steady-state current as a function of bias voltage and temperature [$I=f(V,T)$] yield a parabolic current-voltage law and a linear conductance-temperature dependence. These results are unusual, but by using a numerical approximation they may be interpreted as arising from a network of nonlinear tunnel junctions. The observation of large oscillations in the second-derivative current-voltage spectra near zero bias voltage suggests a resonant tunneling process between localized states a few meV below the insulator conduction-band edge.

I. INTRODUCTION

Charge transport in discontinuous metal films (gold island films) has been an active area of study for more than two decades.¹ More recently, the subject has been stimulated by the interest in localization² and the increasing interest in the unique properties of submicrometer particles.³ This has led to the notion of a different state of matter, viz., the granular state,⁴ which on a phase diagram resides somewhere between the amorphous phase and a polycrystalline phase. Such films are easily prepared experimentally by condensation from the vapor phase on to a suitable substrate. The most widely studied granular or island film has been gold because of its chemical stability and freedom from multilayer oxidation. Some of the earliest work on nucleation and growth used such films, and basic studies of charge transport in discontinuous structures used gold island films. However, the electronic structure of submicrometer grains has yet to be fully established, hence the proliferation of work in this area.

Since the pioneering studies of Neugebauer and Webb,⁵ and Hill,⁶ the charge-transport mechanism in gold island films has been accepted to be thermally activated electron tunneling between islands which are separated by a few nanometers. Deviations from this theory have been considered in terms of traps present in the isolating gap between the islands⁷ and high-field effects.⁸ However, the tunnel currents for a simple metal-insulator-metal (MIM) structure is critically dependent on the gap width. This and other dependent parameters such as the insulator permittivity, chemical state of the oxide, and electrode structure are usually not known very precisely. It follows that the comparison between theory and experiment, even for the simplest of tunnel junctions, has never been very reliable.

A particular source of difficulty in the study of gold island films originates from the statistical distribution of island sizes and interisland gaps. In the tunneling theory applied to such films only one or two potential barriers are considered and these are assumed to be identical. This is clearly not the case in practice, since the island density may be as large as 10^{12} cm⁻² and the islands have a sta-

tistical size distribution. For these reasons a different approach has been considered based on percolation theory.¹ The current state of this approach is limited to considering a distribution of *linear* resistors or diodes which predict a power-law dependence of conductivity with potential.⁹ The fundamental charge-transport mechanisms may therefore be varied and hidden by the statistical distributions of islands. Indeed, experimental results are found to vary considerably and several different models may be chosen to fit experimental data.

One method employed to identify tunneling as a transport mechanism in superconducting MIM junctions is to look for the sharp rise in current which occurs at the critical gap potential or to look for resonant peaks due to phonon vibrations or inelastic tunneling with impurities.¹⁰ Such effects have not previously been investigated in order to validate the theory of tunneling in gold island films.

In this paper, current-voltage and small signal conductance-voltage measurements have been obtained from gold island films at the liquid-helium temperature and above. An empirical analysis of these results yields a parabolic current-voltage law. The assumption of nonlinear transport between islands leads to a very interesting nonlinear network analog, which unfortunately is virtually impossible to solve analytically. Numerical solutions may be available, and in this work we briefly consider the case of a random two-dimensional distribution of highly nonlinear tunneling junctions. This leads to a parabolic I - V characteristic which is nearly independent of the exponential tunneling terms.

Second-derivative current-voltage measurements were also obtained at low temperatures. These results show large oscillations close to zero bias which are considered to arise from resonant tunneling with localized states a few meV below the insulator conduction-band edge.

II. EXPERIMENTAL

A. Specimen preparation

The techniques employed in the preparation of submicrometer-gap gold island films has been described

elsewhere.^{11,12} Briefly, the specimens were prepared in technical vacuum ($\sim 10^{-6}$ Torr) by the thermal evaporation of gold on to previously cleaned silica substrates. Impurity effects were analyzed by inelastic electron tunneling spectroscopy (IETS) as discussed below. A semicontinuous gold film was first produced between two gold electrodes spaced 0.5 mm apart on the silica substrate. A narrow gap was then formed in the semicontinuous film by voltage-controlled electromagnetism. This technique produced a narrow gap (less than $1 \mu\text{m}$ wide) running parallel to the gold electrodes containing a gold island density of about $8 \times 10^{10} \text{ m}^{-2}$. After preparation the samples were transported in air to a liquid-helium Dewar. Three samples were analyzed during each run. The adsorbed impurity layer was investigated by fabricating a separate Al-Pb tunnel junction and obtaining inelastic tunneling spectra using the same equipment as for the gold island specimens. We observed the broad resonances due to hydrocarbon impurity adsorption.¹⁰ We would expect similar impurity adsorption on the gold island samples. However, the results of interest in this work were located close to zero bias well below the hydrocarbon resonances.

B. Electrical measurements

The electrical measurements were performed using harmonic detection and lock-in techniques similar to those used in (IETS).¹⁰ In our method the current was measured directly using a current-to-voltage converter ($I-V$) in Fig. 1. In this case the nonlinear current through the junction may be expanded as a Taylor series,

$$I(V) = I(V_0) + (V - V_0) \left. \frac{dI}{dV} \right|_{V_0} + \frac{1}{2!} (V - V_0)^2 \left. \frac{d^2I}{dV^2} \right|_{V_0} + \dots, \quad (1)$$

where $I(V_0)$ is the steady-state dc component and $V - V_0$ is the modulation voltage. Experimentally, $V - V_0$ is a pure sine wave expressed by

$$V - V_0 = v_{\text{mod}} \cos \omega t. \quad (2)$$

In this work, $V_0 = V_b$ is the bias potential derived from a ramp generator. The output from the oscillator is mixed with the ramp and the resultant signal applied to the test specimens. The amplitude (v_{mod}) was fixed as 9 mV unless otherwise stated and the signal frequency was 800 Hz selected to give the optimum signal-to-noise ratio.

Substituting Eq. (2) into (1) yields

$$I(V) = I_0 + v \cos(\omega t + \phi) \left. \frac{dI}{dV} \right|_{V_0} + \frac{1}{4} v^2 [1 + \cos 2(\omega t + \phi)] \left. \frac{d^2I}{dV^2} \right|_{V_0} + \dots, \quad (3)$$

where ϕ is a phase shift due to the junction capacitance. The experiment consisted of tuning to the first and second harmonics of the detected current signal using lock-in amplifiers (LIA1 and LIA2) in Fig. 1. The outputs from

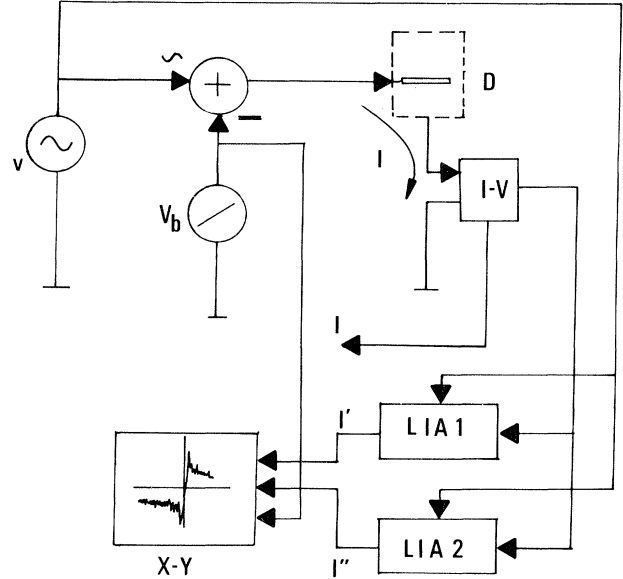


FIG. 1. A schematic diagram of the experimental arrangement for obtaining the first and second derivative (I' and I'' , respectively) of the current through the specimen (I). The modulating source is $V = V_{\text{mod}} \cos \omega t$, where $V_{\text{mod}} = 9 \text{ mV}$ and $\omega = 2\pi f$, where $f = 800 \text{ Hz}$. The bias potential (V_b) is mixed with V and applied to the specimen contained in the Dewar (D). The current through the specimen is converted to a voltage ($I-V$) and applied to two lock-in amplifiers, LIA1 and LIA2. These yield dc levels proportional to the first and second derivatives, respectively, which are applied directly to an X-Y recorder where the X axis is proportional to the dc bias level.

these lock-in amplifiers consisted of dc levels directly proportional to the first and second derivatives of the junction current as expressed by Eq. (3). The small signal conductance and its derivative are then defined by

$$g = \left. \frac{dI}{dV} \right|_{V_0} \quad \text{and} \quad g' = \left. \frac{d^2I}{dV^2} \right|_{V_0},$$

respectively. Absolute values of g in siemens were obtained by substituting the junction test specimens for resistances of known values. This procedure also ensured that the lock-in amplifiers were tuned to the purely resistive component of the junction impedance.

III. EXPERIMENTAL RESULTS

A. Current-voltage characteristics

A typical current-voltage family of characteristics is shown in Fig. 2. This is raw data traced directly from chart recordings. The noise in the curves increased slightly with increasing temperature. This noise was removed during tracing of the curves. The measurements were obtained by repeated recording of the $I-V$ characteristics while the temperature increased from 10 K to room temperature. The temperature was controlled by means of a heater mounted inside the Dewar. The curves were calibrated with 1% external resistors and the recording of 100-k Ω resistance is shown appended to Fig. 2.

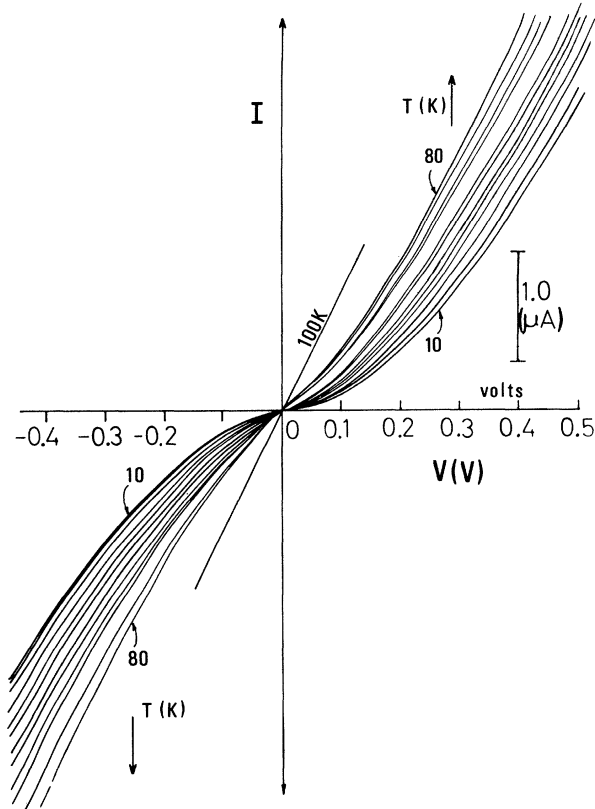


FIG. 2. Typical family of I - V characteristics obtained over a temperature range of 10–80 K. The straight line was obtained from a resistor used for calibration purposes. Details of the temperature results are shown in Fig. 3(a).

B. Current-temperature characteristics

Figures 3(a) and (b) show current-versus-temperature plots for two different specimens. At low temperatures this shows a linear current-temperature relationship, but with the slope increasing with increasing bias voltage.

C. Conductance-voltage characteristics

The small signal conductance-voltage curves shown in Fig. 4 were obtained simultaneously with the current curves in Fig. 1. These two sets of data have been separated for clarity. The small signal conductance was obtained by the harmonic detection methods described previously. Calibration in microsiemens was achieved by the use of 1% tolerance resistors, and the dashed line in Fig. 4 shows a value of $1 \text{ M}\Omega$. All other calibration points also yielded straight lines for standard resistors showing that the non-linear effects were due entirely to the devices under test. The curvature in these g - V plots on a nearly linear background is the subject of further analysis by means of second-derivative current-voltage measurements (subsection F).

D. Conductance-temperature characteristics

The variation of conductance with temperature is shown in Figs. 5(a) and (b) for two different specimens.

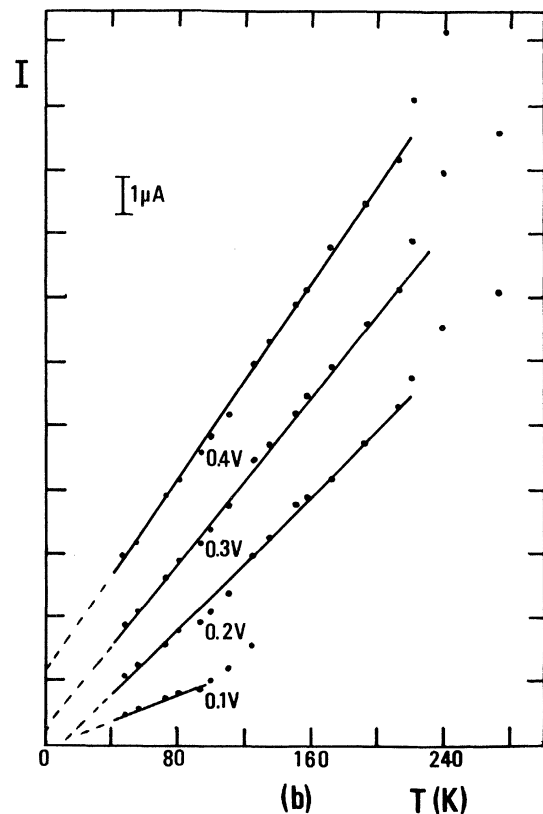
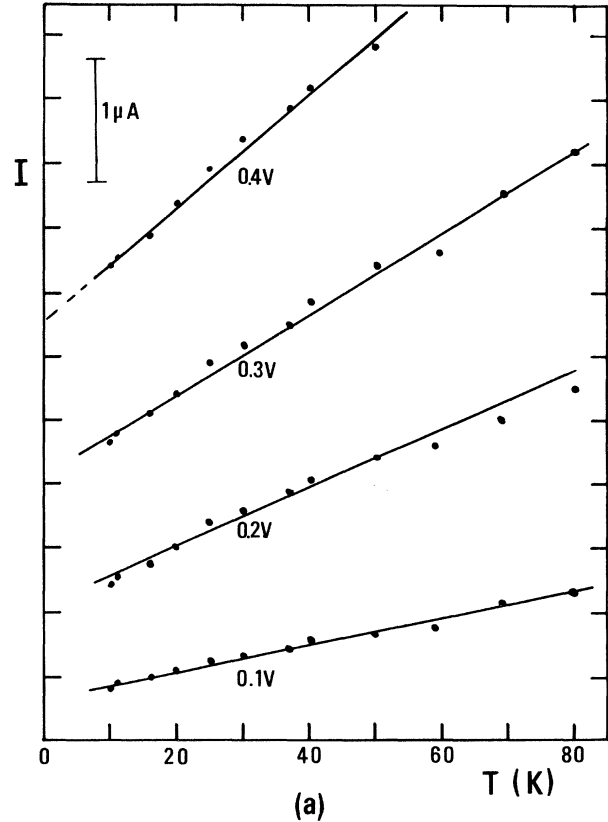


FIG. 3. Current-temperature characteristics for constant bias potentials. (a) Results obtained from positive quadrant of Fig. 2. (b) Results obtained from a second specimen over an extended temperature range.

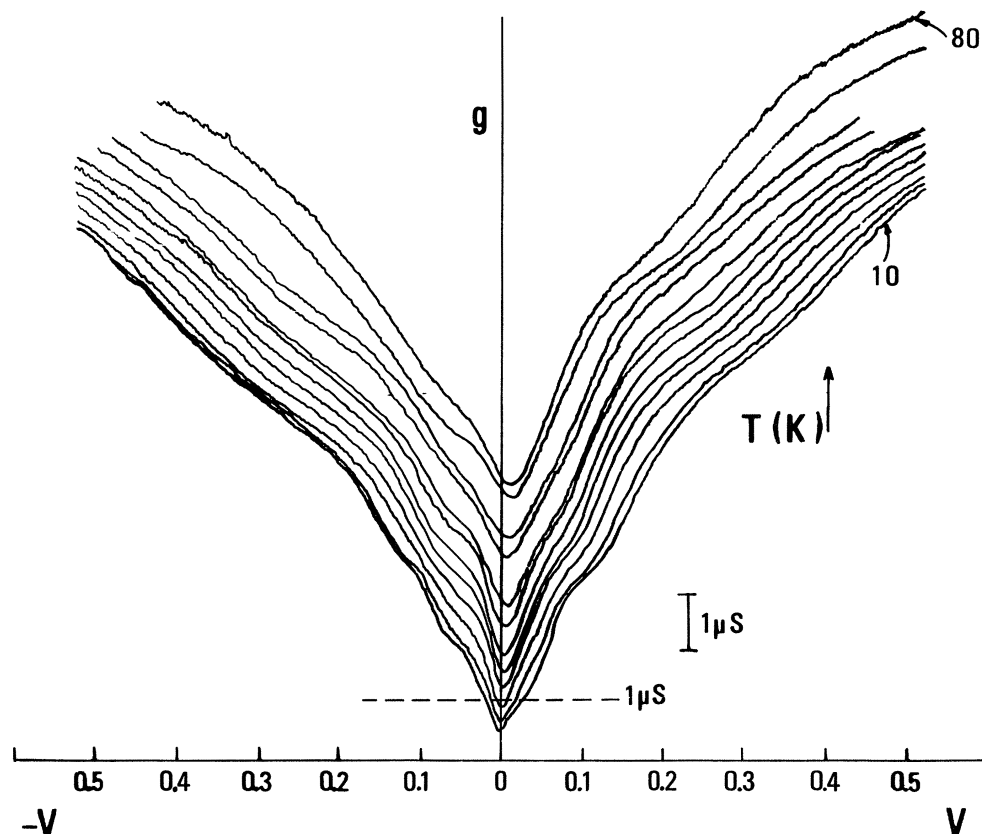


FIG. 4. Small signal conductance-voltage characteristics of the I - V curves of Fig. 2. The dashed line corresponds to a $1.0\text{-}\mu\text{S}$ calibration point. The curves were obtained over the same temperature range as Fig. 2 (10–80 K).

This shows that for the mid-temperature range of the analysis the relationship is linear. Deviations from linearity occur for nonzero-bias potentials and temperatures below about 30 K. At higher temperatures, 220°C in Fig. 5(a) and 30 K in Fig. 5(b), there appears to be some peaks in the g - T characteristic. An empirical analysis is considered in the following section.

E. Empirical considerations

Assuming that there are no structural or chemical changes in the discontinuous film, the steady-state current I may be expressed as a function of bias potential V and temperature T only,

$$I = f(V, T). \quad (4)$$

The total derivative is

$$dI = \left. \frac{\partial I}{\partial V} \right|_T dV + \left. \frac{\partial I}{\partial T} \right|_V dT. \quad (5)$$

The term

$$g_T = \left. \frac{\partial I}{\partial V} \right|_T$$

is the small signal conductance at constant temperature. In the preceding work the following linear relationships occurred.

From Figs. 3 and 4, for constant bias potentials,

$$I|_V = m_1 T + I_0, \quad (6)$$

$$g|_V = m_2 T + g_{0V}. \quad (7)$$

From Figs. 4 and 7, for constant temperature,

$$g|_T = m_3 V + g_{0T}, \quad (8)$$

where m_1 , m_2 , m_3 , I_0 , g_{0V} , and g_{0T} are constants. Substituting in Eq. (5) yields

$$dI = (m_3 V + g_{0T}) dV + m_1 dT. \quad (9)$$

Hence,

$$I = \int (m_3 V + g_{0T}) dV + \int m_1 dT. \quad (10)$$

Assuming g_{0T} originates from a leakage conductance, then after setting $g_{0T} = 0$,

$$I = m_3 (V^2/2) + m_1 [T(V) - T(0)]. \quad (11)$$

This equation would be expected to hold over the linear regions of the above results. However, it would not be expected to hold for bias potentials approaching 0 V, and for higher temperatures.

A plot of I vs V^2 is shown in Fig. 6, and the square law is shown to be valid for this linear region. Figure 7 shows the I - V and g - V results obtained from another specimen recorded over a larger voltage range. The conductance is

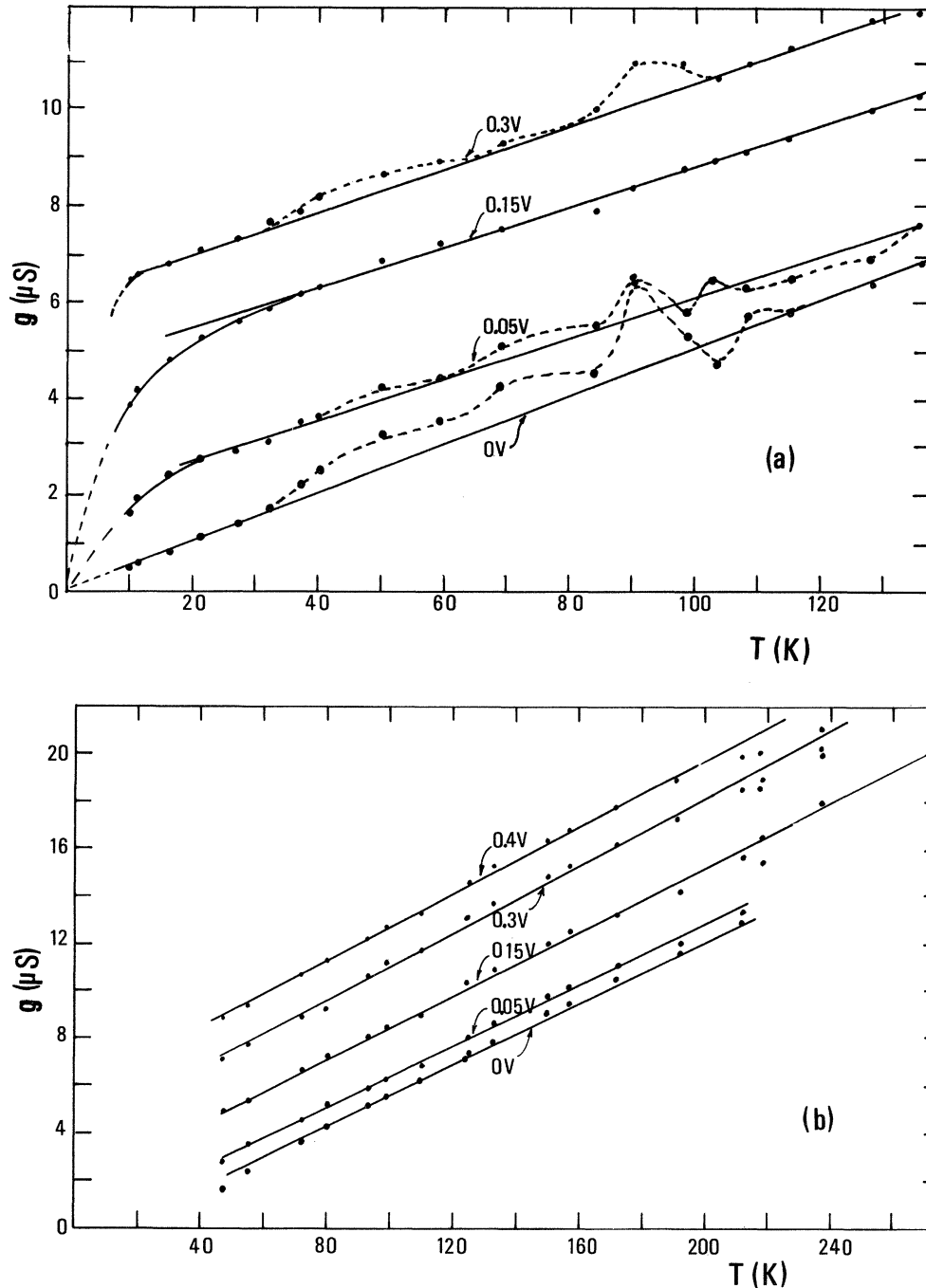


FIG. 5. (a) Conductance-temperature characteristics obtained from positive quadrant of Fig. 4 including higher-temperature measurements. (b) Results obtained from another specimen.

seen to be approximately linear above 0.1 V, and the current shows an excellent parabolic voltage dependence.

F. Conductance oscillations

Small-signal-conductance measurements and their derivative obtained from a discontinuous gold island film are shown in Fig. 8. The conductance increases in linear stages for plus and minus bias potentials but the plots are

not perfectly symmetrical around zero bias. The derivative shows peaks on a steplike background for both bias polarities. This cyclic behavior was confined to a bias region of about ± 100 mV and the signal noise increased rapidly above this potential. Peak width and peak separation were found to depend sensitively on the temperature and magnitude of the applied bias. It was found to be possible to "anneal" the specimens by current heating. This was performed by applying progressively increasing bias voltages to the specimens, in a procedure similar to

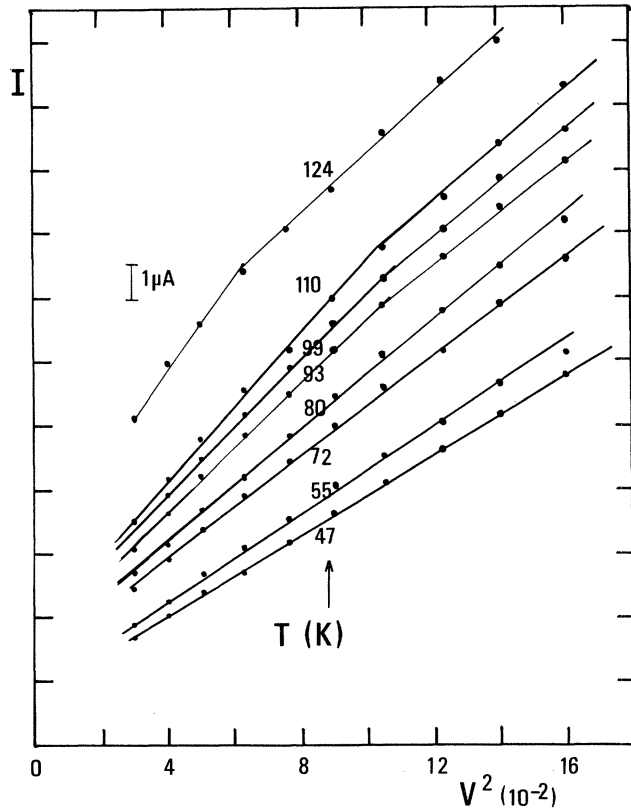


FIG. 6. Plots of I vs V^2 for constant temperatures.

that used by Konkin and Adler.¹³ The results of such a procedure are shown in Fig. 9. After annealing, several of the peaks were absent. However, the peak close to zero bias increased in magnitude, the background increased, and there remains a significant shoulder on the high-energy side of the zero-bias peak.

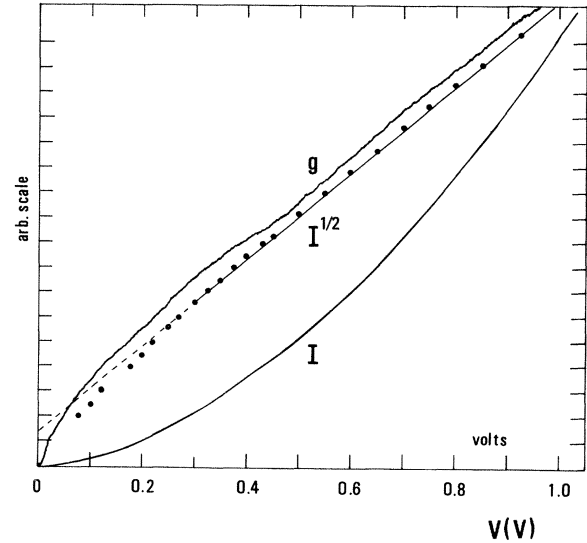


FIG. 7. Plots of g vs V , I vs V , and computed values of $I^{1/2}$ vs V .

IV. DISCUSSION

The current-voltage characteristics obtained in this work yield a power-law dependence over a wide temperature range. These observations are found to be in agreement with previous work for specimens prepared under slightly different conditions with the specimens held in vacuum during measurement and the temperature range limited to a maximum of 77 K. In the previous work, however, the temperature results were interpreted in terms of an Arrhenius temperature dependence.¹⁴ In the more extensive low-temperature measurements reported here, both the current and the conductance have a nearly linear temperature dependence. This is found to be consistent

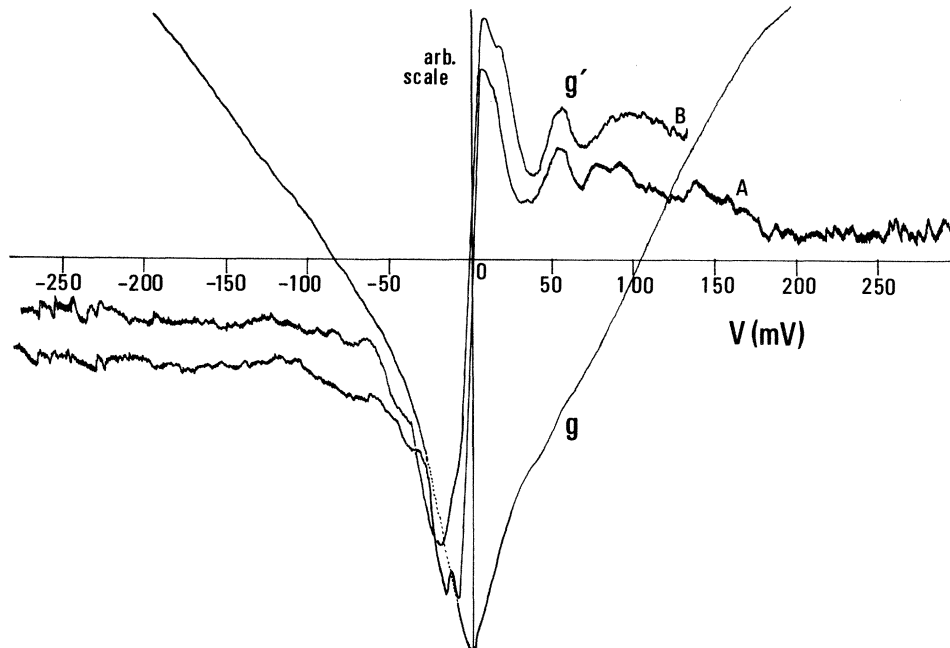


FIG. 8. First- and second-derivative current-voltage spectra (g and g' , respectively) obtained at 10 K. Linear regions occur in the g characteristics and peaks are observed in the g' scans. Curve A is the first scan and curve B is a repeat scan.

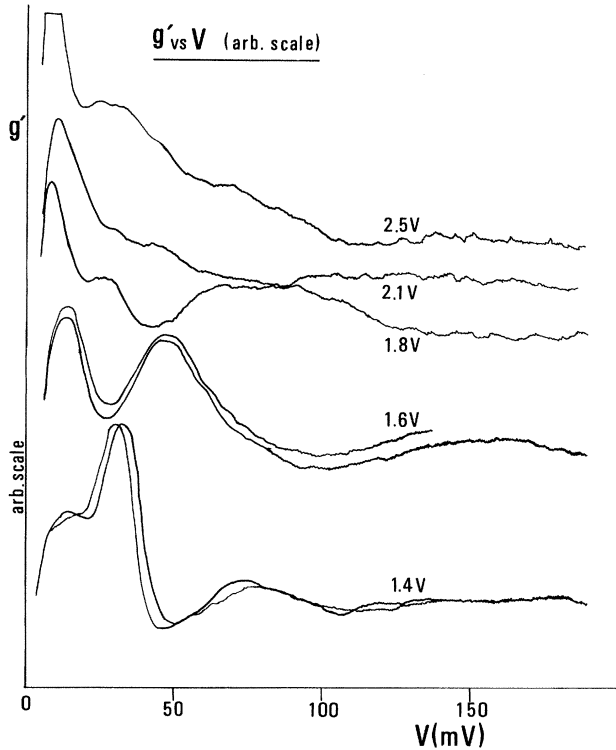


FIG. 9. Effects of “annealing” on peaks in the g' and V spectra. The annealing was achieved by increasing the power dissipated by the specimen (indicated on each scan by the maximum applied potential during annealing). The annealing process leads to a change in the spectra, except for the peak close to zero bias which remains at a fixed energy for constant temperature. This peak was found to shift to a higher energy and to broaden for increasing temperatures. The bottom two scans show repeat traces indicating the repeatability after annealing.

with the empirical analysis given in Sec. III E. Such observations do not appear to be consistent with tunneling theories proposed for charge transport in gold island films. However, for small values of bias applied to asymmetric MIM tunnel junctions the conductance has been observed to vary nearly linearly with bias voltage. This was considered to be due to impurity excitation effects, which “fill in” the conductance minimum.¹⁵ In the discussion which follows, it is suggested that the results obtained from gold island films are consistent with a tunneling model. The new measurements obtained in this work which show oscillations in the second-derivative current-voltage characteristics further support a tunneling model.

A. Parabolic law

Consider first the high-field tunneling situation where the current is described by the Fowler-Nordheim equation,

$$I = \alpha_1 V^2 \exp \left[-\frac{\alpha_2}{V} \right], \quad (12)$$

where α_1 and α_2 contain parameters concerning the barrier

height and geometrical factors. For high potentials V the current-voltage law would be expected to tend toward a square-law form and the conductance-voltage curve would become linear. However, this approximation applies only for high potentials and a single junction. For the gold island films a square-law behavior is observed at relatively low bias values. The actual potential difference between islands would be expected to be several times less than the bias voltage. The above considerations, however, would apply if a *single gap* dominated the conduction process. The problem becomes one of considering a two-dimensional matrix of nonlinear resistors, and such a problem can only be approached numerically or by fabricating a physical model consisting of an array of tunnel junctions. The numerical approach is briefly considered below. A more detailed account of both techniques is to be published later.

B. Numerical approximation

This approach uses a two-dimensional network of nonlinear resistors to solve for the nodal current vector,

$$\vec{J}_n = \vec{y}_n \cdot \vec{u}_n, \quad (13)$$

where \vec{y}_n is an $n \times n$ nodal admittance matrix which contains information about the topology and impedances of the network; \vec{u}_n is a column vector with n elements for which u_{nj} is the potential at the j th node. In the gold island problem the nodes are situated at the islands and the model consists of deciding on the island distribution and spacing, and solving the matrix equations. For a small number of islands (about nine) and spacings which vary by only a few percent, it is found that, for an interisland nonlinearity given by Eq. (12), the total current obeys a similar law. However, for a larger density of islands and larger variation on spacings the total current varies as $I \propto V^n$ where $n \cong 2$.

C. Temperature dependence

Experimentally it is found that gold island films have a negative temperature coefficient of resistance and an Arrhenius plot yields a small activation energy. This energy is thought to be the average energy required to charge an island and is equivalent to the Coulomb energy $\frac{1}{2}qV$. Zeller and Giaver¹⁶ also found a linear conductance-temperature dependence for small Sn particles embedded in an oxide-MIM tunnel junction. These authors considered the zero-bias conductivity to be given by

$$\sigma(0, T) \propto \int_0^\infty e^{-eV_c/kT} dV_c, \quad (14)$$

for single-electron-charging of the islands, so that $\sigma(0, T) \propto T$, which is the type of behavior observed experimentally for gold island films. If the bias voltage is not zero there is a distribution of potentials and a numerical analysis is necessary.

D. Conductivity oscillations

Further evidence to support a tunneling model is the occurrence of oscillations in the second-derivative current

spectra. Two forms of oscillatory behavior were observed. The first kind appeared at a few mV from zero bias in both forward and reverse current directions. The shift of this peak to higher energies, and the peak-broadening effect as the temperature increased, are essentially similar to those observed for trap-assisted resonant tunneling in MIM junctions.¹⁷⁻¹⁹ However, the peak width was found to be several times the value of $5.4kT$ expected for resonant tunneling. This large width may be due to the relatively large modulation voltage of 9 mV peak used in this measurement.

The other kind of oscillations, observed in Fig. 9, could be suppressed by an annealing process. This suggests that the traps giving rise to these oscillations were removed, while the oscillation close to zero bias was due to a permanent trap located close to the insulator conduction-band edge.

V. CONCLUSIONS

The parabolic current law and linear conductance-temperature behavior are rather surprising results which

differ from other observations on gold island films. However, the linear conductance-temperature behavior has been observed for MIM superconducting tunnel junctions, and we show in this work that on gold islands the results are consistent with a tunneling model. The precise nature of the tunneling path is still uncertain, but the oscillatory behavior observed in the second-derivative current spectra suggests that the tunneling path is via fixed states and mobile states located a few meV below the conduction-band edge.

ACKNOWLEDGMENTS

A large proportion of the work was carried out in the Institut für Angewante Physik, Technische Hochschule Darmstadt, Darmstadt, and the author would like to acknowledge the considerable support and interest by Dr. Nick Sotnik and Professor H. Pagnia. The author wishes also to acknowledge the Deutscher Akademischer Austauschdienst (DAAD) for providing a grant to pursue this work.

¹J. E. Morris and T. J. Coutts, *Thin Solid Films* **47**, 3 (1977).

²Y. Bruynseraede, M. Gijs, C. Van Haesendonck, and G. Deutscher, *Helv. Phys. Acta* **56**, 37 (1983).

³J. Friedel, *Helv. Phys. Acta* **56**, 507 (1983).

⁴H. Gleiter, in *Proceedings of the Ninth International Vacuum Congress and the Fifth International Conference on Solid Surfaces, Madrid, 1983*, edited by J. L. del Segovia (Asociacion Española Del Vicio y sus Aplicaciones, Madrid, 1983), p. 397.

⁵C. A. Neugebauer and M. B. Webb, *J. Appl. Phys.* **33**, 74 (1962).

⁶R. M. Hill, *Proc. R. Soc. London, Ser. A* **309**, 377 (1969).

⁷M. Celasco, A. Masoero, P. Mazzetti, and A. Stepanescu, *Phys. Rev. B* **17**, 2553 (1978).

⁸K. Uozoumi, M. Nishiura, and A. Kinbara, *J. Appl. Phys.* **48**, 818 (1977).

⁹S. Redner and P. R. Mueller, *Phys. Rev. B* **26**, 5293 (1982).

¹⁰R. G. Keil, T. P. Graham, and K. P. Roenker, *Appl. Spec-*

trosc. **30**, 1 (1976).

¹¹A. Rahman and M. S. Raven, *J. Phys. D* **13**, 701 (1980).

¹²R. Blessing and H. Pagnia, *Thin Solid Films* **52**, 333 (1978).

¹³M. K. Konkin and J. G. Adler, *J. Appl. Phys.* **53**, 5057 (1982).

¹⁴M. S. Raven, in *Proceedings of the Eighth International Vacuum Congress, Cannes, France 1980*, edited by F. Abélès, and M. Croset (Societe Francaise Du Vide, Paris, 1980), Vol. 1, p. 619.

¹⁵W. F. Brinkman, R. C. Dynes, and J. M. Rowell, *J. Appl. Phys.* **41**, 1915 (1970).

¹⁶H. R. Zeller and I. Giaever, *Phys. Rev.* **181**, 789 (1969).

¹⁷X. Aymerich-Humet and F. Serra-Mestres, *Solid State Commun.* **36**, 551 (1980).

¹⁸X. Aymerich-Humet and F. Serra-Mestres, *Phys. Status Solidi A* **54**, 655 (1979).

¹⁹J. G. Adler and J. Strauss, *Phys. Rev. B* **13**, 1377 (1976).